J Neurophysiol 98: 3349–3359, 2007.
First published October 17, 2007; doi:10.1152/jn.00898.2007.

Synaptic Vesicle Endocytosis at a CNS Nerve Terminal: Faster Kinetics at Physiological Temperatures and Increased Endocytotic Capacity During Maturation

Robert Renden and Henrique von Gersdorff
The Vollum Institute, Oregon Health and Science University, Portland, Oregon

Submitted 10 August 2007; accepted in final form 6 October 2007

Renden R, von Gersdorff H. Synaptic vesicle endocytosis at a CNS nerve terminal: faster kinetics at physiological temperatures and increased endocytotic capacity during maturation. *J Neurophysiol* 98: 3349–3359, 2007. First published October 17, 2007; doi:10.1152/jn.00898.2007. Synaptic vesicle membrane must be quickly retrieved and recycled after copious exocytosis to limit the depletion of vesicle pools. The rate of endocytosis at the calyx of Held nerve terminal has been measured directly using membrane capacitance measurements from immature postnatal day P7–P10 rat pups at room temperature (RT: 23–24°C). This rate has an average time constant of tens of seconds and becomes slower when the amount of exocytosis (measured as capacitance jump) increases. Such slow rates seem paradoxical for a synapse that can operate continuously at high-input frequencies. Here we perform time-resolved membrane capacitance measurements from the mouse calyx of Held in brain stem slices at physiological temperature (PT: 35–37°C), and also from more mature calyces after the onset of hearing (P14–P18). Our results show that the rate of endocytosis is strongly temperature dependent, whereas the endocytotic capacity of a nerve terminal is dependent on developmental stage. At PT we find that endocytosis accelerates due to the addition of a kinetically fast component (time constant: $\tau = 1$–2 s) immediately after exocytosis. Surprisingly, we find that at RT the rate of endocytosis triggered by short (1- to 5-ms) or long (≥10-ms) depolarizing pulses in P14–P18 mice are similar ($\tau \approx 15$ s). Furthermore, this rate is greatly accelerated at PT ($\tau \approx 2$ s). Thus endocytosis becomes faster and less saturable during synaptic maturation, making the calyceal terminal more capable of sustaining prolonged high-frequency transmitter release.

INTRODUCTION

Synaptic vesicles are reused following exocytosis to sustain chemical transmission at synapses (Rizzoli and Jahn 2007; Schweizer and Ryan 2006; Südhof 2004). Studies using membrane capacitance have determined the rate of endocytosis in neuroendocrine cells (Betz and Angleson 1998; Smith and Neher 1997), in sensory neurons (Moser and Beutner 2000; Rieke and Schwartz 1996), and in large nerve terminals (Hallermann et al. 2003; Sun and Wu 2001; von Gersdorff and Matthews 1994). For small central bouton-type synapses, optical measurements have been used to probe the vesicle cycle (Aravanis et al. 2003; Ferguson et al. 2007; Gandhi and Stevens 2003). These studies have generally found that activity-dependent endocytosis is composed of at least two kinetically distinct components: one that occurs after brief stimuli with fast rates of hundreds of milliseconds to seconds, and another slower form that occurs after stronger stimulation with slower rates of tens of seconds (LoGiudice and Matthews 2007; Wu 2004). However, the physiological relevance of these two separate modes of endocytosis—as well as their molecular mechanisms and possible modulation–is still under debate.

The calyx of Held, a large CNS presynaptic terminal, is amenable not only to direct intracellular recordings but also to dye imaging studies (de Lange et al. 2003; Sun and Wu 2001). Endocytosis at this synapse occurs with a time constant of several seconds, becoming slower as the stimulus duration or strength increases (Sun and Wu 2001; Yamashita et al. 2005). It is dependent on guanosine triphosphate (GTP) and dynamin (Yamashita et al. 2005), but independent of free intracellular Ca^{2+} ($[Ca^{2+}]_i$; Sun et al. 2002). In addition, the rate of endocytosis is dependent on the magnitude of previous exocytosis (Sun et al. 2002; Yamashita et al. 2005). However, repetitive strong stimulation recruits an additional calmodulin-sensitive fast component of endocytosis, dependent on high $[Ca^{2+}]_i$ elevations (Wu et al. 2005).

These previous studies used postnatal day (P) 7 to P11 rat pups. However, rats and mice are deaf before P12 (Blatchley et al. 1987) and their calyx of Held synapse is developmentally immature (Taschenberger et al. 2002). Additionally, most experiments using this synapse were performed at room temperature. Previous reports have shown that the rate of endocytosis is very sensitive to temperature, with up to a threefold increase in the rate at physiological temperatures (Fernandez-Alfonso and Ryan 2004; Johnson et al. 2005; Micheva and Smith 2005; Teng and Wilkinson 2003). It is thus likely that the kinetics of endocytosis at this calyceal synapse have been underestimated.

Here we report measurements of endocytosis from the young murine calyx of Held (P7–P10) at physiological temperature (PT, 35–37°C) and from older mice where the calyx is more functionally mature (P14–P18). In immature mouse calyces at RT (23–24°C), our results agree well with previous reports from the rat calyx; however, we see a two- to threefold increase in the rate of endocytosis at PT, regardless of stimulation intensity. Unexpectedly, in more mature mouse terminals endocytosis rates were similar for short [single action potential (AP)–like] pulses and long depolarizing pulses, consistent with the hypothesis that retrieval capacity is increased during synaptic maturation, perhaps due to more abundant endocytotic proteins. In these terminals, physiological temperature further

Address for reprint requests and other correspondence: H. von Gersdorff, The Vollum Institute, L-474, Oregon Health and Science University, 3181 Southwest Sam Jackson Park Road, Portland, OR 97239 (E-mail: vongersd@ohsu.edu).

The costs of publication of this article were defrayed in part by the payment of page charges. The article must therefore be hereby marked "*advertisement*" in accordance with 18 U.S.C. Section 1734 solely to indicate this fact.

 0022-3077/07 $8.00 Copyright © 2007 The American Physiological Society

accelerated membrane retrieval twofold, even for long (20- to 30-ms) depolarizations that triggered copious exocytosis. The ability to faithfully follow high-frequency firing increases with age and temperature (Taschenberger and von Gersdorff 2000), and we thus propose that this may be partly due to a greater capacity to quickly retrieve fused vesicular membrane and recycle vesicles in mature synapses.

METHODS

Slice preparation

C57/bl6J mice (The Jackson Laboratory, Bar Harbor, ME) postnatal day P7 to P18 old were used in this study. Young (P7–P10) mice had closed eyes and lacked a startle response to brief auditory stimulus (e.g., hand clap). Mice in the older age group (P14–P18) had open eyes and showed a response to auditory stimuli. After decapitation, the brain stem was quickly removed from the skull and submerged in ice-cold saline, containing the following (in mM): 125 NaCl, 2.5 KCl, 3 $MgCl_2$, 0.1 $CaCl_2$, 25 glucose, 25 $NaHCO_3$, 1.25 NaH_2PO_4, 0.4 ascorbic acid, 3 myo-inositol, and 2 Na-pyruvate [pH 7.3–7.5 when bubbled with carbogen (95% O_2-5% CO_2); osmolality was 310–315 mOsm]. Transverse slices were made 150–160 μm thick for presynaptic recordings and 200 μm thick for postsynaptic recordings, containing the medial nucleus of the trapezoidal body (MNTB) using a vibratome (VT1000; Leica, Bannockburn, IL). Slices were then transferred to an incubation chamber containing normal saline bubbled with carbogen, maintained for 60 min at 35°C and thereafter at room temperature (22–25°C) until used for recording. Normal saline was the same as slicing saline, but with 1 mM $MgCl_2$ and 2 mM $CaCl_2$.

Electrophysiology

Slices were transferred to a recording chamber and perfused at 1–3 ml/min with a normal saline bath solution. Solution was warmed to 35–37°C in some experiments using an in-line heater (Warner Instruments, Hamden, CT). Recordings at physiological temperature were initiated 10 min to 1 h after the slice was reequilibrated at 35–37°C, unless otherwise noted (e.g., Fig. 2). Slices were visualized using infrared differential interference contrast microscopy (Leica) and a ×40 or ×63 water-immersion objective, and observed on a television screen using a CCD camera (Hamamatsu Photonics, Bridgewater, NJ). Ionotropic glutamate receptors (α-amino-3-hydroxy-5-methyl-4-isoxazolepropionic acid and *N*-methyl-D-aspartate) were blocked by bath perfusion of 50 μM D-2-amino-5-phosphonovaleric acid and 10 μM 2,3-dihydroxy-6-nitro-7-sulfamoyl-benzo[f]quinoxaline-2,3-dione (NBQX) or 6-cyano-7-nitroquinoxaline-2,3-dione (CNQX), respectively; glycine receptors by 0.5 μM strychnine; and γ-aminobutyric acid receptors by 10 μM bicuculline. This treatment eliminated the possibility of capacitatively coupled postsynaptic receptor conductances (Borst et al. 1995; Forsythe 1994; Wolfel and Schneggenburger 2003). Ca^{2+} currents were isolated by blocking I_{Na} with 1 μM tetrodotoxin (TTX) and I_K with 5 mM tetraethylammonium (TEA) in the bath solution. The pipette internal solution for presynaptic calcium current and capacitance recordings contained the following (in mM): 130 Cs-gluconate, 15 CsCl, 5 Na_2-phosphocreatine, 10 HEPES, 0.2 EGTA, 20 TEA-Cl, 4 Mg-ATP, and 1 GTP (pH adjusted to 7.3 with CsOH, and osmolality of 305–310 mOsm).

Pipettes were pulled from thick-walled borosilicate glass (Sutter Instrument, Novato, CA) with a Sutter P-97 electrode puller to open tip resistances of 4–8 MΩ for presynaptic recordings. Pipette tips were coated with dental wax to reduce pipette capacitance. Pipette pressure was monitored with a manometer, but was not adjusted; hydrostatic pressure was zero or slightly negative (Heidelberger et al. 2002). Data were acquired at 10- to 25-μs sampling rate, using an EPC-9 patch-clamp amplifier controlled by Pulse 8.4 software (HEKA Elektronik, Lambrecht/Pfalz, Germany), filtered on-line at 2.9 kHz, and run by a Power Macintosh G3 computer (Apple Computers, Cupertino, CA). Step depolarizations were to 0 mV, unless stated otherwise.

Presynaptic terminals were voltage clamped at −80 mV, and access resistance was compensated ≤75%, such that residual series resistance (R_s) was usually 7–10 MΩ. Terminals with membrane resistance (R_m) <1 GΩ were discarded from analysis. Membrane capacitance was calculated from a 1-kHz, 30-mV-amplitude sine wave on the holding potential, using the software lock-in capability of the EPC-9 amplifier (Gillis 1995). The reversal potential was assumed to be 0 mV. Membrane capacitance (C_m) was not measured during step depolarizations (Sun and Wu 2001; Taschenberger et al. 2002), and a minimum of 30 s was allowed between depolarizations to allow for complete recovery from synaptic depression (Kushmerick et al. 2006).

Calyces of young animals can be fit by a single- or two-compartmental passive model, due to the presence of the afferent axon, but this does not significantly alter their exo- or endocytotic properties, as reported previously (Taschenberger et al. 2002; Wu et al. 2005). However, during development, the presynaptic calyx morphology becomes more complex (Taschenberger et al. 2002), which could result in significant filtering and loss of adequate voltage clamp in the terminals of older animals. In animals older than P14, passive membrane capacitance properties nearly always indicated a two-compartmental terminal, which could be adequately fit by a biexponential function (Supplemental Fig. 1*A*).[1] Mean time constants (±SE) were τ_{fast} = 0.19 ± 0.01 ms, which carried 82% of the current, and τ_{slow} = 2.1 ± 0.1 ms (n = 56 calyx terminals). These numbers match well with those reported for passive C_m of P12–P14 rat calyces (Taschenberger et al. 2002). In addition, the sine wave used for calculation of membrane capacitance was not significantly filtered by the complex morphology because similar exocytotic increases in C_m were observed for depolarizations when the sine-wave frequency was varied between 500 Hz and 2 kHz (Supplemental Fig. 1*B*). Thus accurate measurement of membrane capacitance in the presynaptic terminal of older animals could still be achieved using a 1-kHz sine wave, even in the presence of complex terminal morphology.

Drugs and reagents

All salts, as well as NBQX, strychnine, kynurenic acid, and cypermethrin were purchased from Sigma (St. Louis, MO). TTX was purchased from Alomone Labs (Jerusalem, Israel). All other pharmacological agents (D-APV, bicuculline, CNQX) were purchased from Ascent Scientific (Weston-Super-Mare, UK).

Analysis

Baseline C_m was linearly corrected for drift 10–20 s before a step depolarization (Horrigan and Bookman 1994). For exocytosis, baseline C_m was measured at 0.5 to 2 s before step depolarization. Exocytosis (or C_m jump) was evaluated as the difference in baseline just before and 0.5 to 1 s after a depolarization, beginning >250 ms after the end of depolarization to avoid depolarization-induced changes in membrane conductance and capacitance artifacts (Yamashita et al. 2005). Presynaptic calcium currents were calculated by P/5 leak subtraction with leak traces acquired just before depolarization.

Long traces that tracked C_m for endocytosis were made using "snapshots" of the membrane capacitance, as reported previously (Sun et al. 2002; Yamashita et al. 2005). Briefly, a 1-kHz sine wave was recorded for 20 ms at a high sampling rate (20 μs) every 500 ms before and after the step depolarization. The calculated C_m was then averaged for each 500-ms time point. This allowed us to accurately

[1] The online version of this article contains supplemental data.

track C_m over the course of 2–3 min after a step depolarization. Endocytosis (or C_m decay) sweeps from a single cell were averaged and fit with a single or double exponential starting immediately (20 ms) after the step depolarization, until the trace returned to baseline values or the end of the sweep. This approach could result in contamination of the first C_m data point after the depolarization step, due to capacitance artifacts that occur <400 ms after the depolarization (Yamashita et al. 2005). However, eliminating the first data point (C_m at 20–40 ms after the step depolarization) from decay fits had only a marginal effect on the time constant at RT. Endocytosis at PT was affected only for long (30-ms) depolarizations, decreasing the weight and increasing the value of the time constant by <1 s for fast endocytosis, but dramatically reduced the measured capacitance jump. The weighted mean decay rate (τ_m) was calculated from the individual exponential time constants (τ_{fast} and τ_{slow}) and their respective amplitude components (A_1 and A_2) as

$$\tau_m = \tau_{fast}[A_1/(A_1 + A_2)] + \tau_{slow}[A_2/(A_1 + A_2)]$$

Most cells used for analysis had two to five sweeps of capacitance at a given step depolarization. Endocytosis was analyzed only in sweeps obtained <10 min after break-in to avoid rundown of responses (Hull and von Gersdorff 2004; Parsons et al. 1994). Ideally, perforated-patch techniques would be implemented for recording capacitance (Price and Trussell 2006). However, this mode of recording typically produces high access resistance (R_s = 30–50 MΩ), which precludes reliable and low-noise C_m recordings (Gillis 1995).

Retrieval rates were calculated by converting the exo–endo relationship from fF/s to SV/s, using a single vesicle capacitance of 61 aF (Wu et al. 2007). Thus ΔC_m (fF)/[τ_m (s)/$C_m$vesicle (fF/SV)] = SV/s. If a linear dependence of endocytosis rate to exocytosis (ΔC_m) was shown, as for immature calyces, values for 1/slope from a linear fit were used. In the case of mature calyceal terminals, where the capacity for endocytosis is increased and there is no relationship between the magnitude of exocytosis and the speed of endocytosis, we used ΔC_m and τ_m values due to short (2-ms) and long (30-ms) depolarizations to estimate retrieval rates for these two conditions.

Data were analyzed off-line and presented using Igor Pro (WaveMetrics, Lake Oswego, OR). Single exponential values are reported for passive cell membrane properties, unless a biexponential fit returned a 50% smaller relative χ^2 value, defined as $(\chi_1^2 - \chi_2^2)/\chi_2^2$, where χ_1^2 is from a monoexponential fit and χ_2^2 is from a biexponential fit. For endocytosis, single exponential values are reported, unless the relative χ^2 value was 15% smaller for a biexponential function. Statistical analyses were performed using Prism 4.0 (GraphPad, San Diego, CA). Means ± SE are reported, unless otherwise noted. Significance is reported as $*P < 0.05$, $**P < 0.01$, and $***P < 0.001$, using appropriate tests.

RESULTS

Previously we reported that capacitance jumps and the refilling rate of the readily releasable pool of vesicles at the calyx of Held increase dramatically at physiological temperature (PT), but we did not discern whether endocytosis was also accelerated at PT (Kushmerick et al. 2006). Here, we examined endocytosis at PT to gain further insight into the factors that may rate limit synaptic vesicle recycling and reuse.

Capacitance measurements at the mouse calyx terminal

Capacitance jumps reflecting Ca^{2+}-dependent exocytosis of synaptic vesicles due to depolarizations lasting 1 to 30 ms were measured in immature calyces (P7–P10), both at room temperature (RT, 22–25°C) and physiological temperature (PT, 35–37°C). The ΔC_m jumps correlate well with cumulative excitatory postsynaptic currents (EPSCs) and total synaptic vesicle release at RT in the rat calyx of Held using deconvolution analysis (Sakaba 2006). Our exocytosis data from mice (Supplemental Fig. 2) also show that longer depolarizations lead to larger Ca^{2+} influx and increasingly larger ΔC_m jumps (Kushmerick et al. 2006). In older mice (P14–P18), exocytosis at RT was greater than that in younger animals for similar Ca^{2+} influx, indicating a larger releasable pool of vesicles and/or increased Ca^{2+} sensitivity, similar to previous reports in more mature rats (Taschenberger et al. 2002). We thus suggest that the basic excitation–secretion coupling parameters, as well as developmental changes in exocytosis capacity, are likely conserved and similar between rats and mice.

EPSCs show significant variability from trial to trial at the calyx of Held (Scheuss et al. 2002). Likewise, exocytosis measured as changes in ΔC_m also shows intertrial variability. Figure 1*A* shows this and an example of the even more substantial variability observed in endocytosis rate from trial to trial (see also Wu et al. 2005). The coefficient of variation (C_v) for the Q_{Ca} (total Ca^{2+} influx charge, measured as an integral of the Ca^{2+} current) of the sweeps shown in Fig. 1*A* was 0.039, whereas the C_v for ΔC_m was 0.149 (Fig. 1*B*). In addition, this figure also illustrates the substantial rundown of membrane retrieval (capacitance decay) after about 10 min following establishment of the whole cell recording configuration, presumably due to dilution of soluble endocytotic proteins from the cytosol by the intracellular patch-pipette solution (Parsons et al. 1994). Endocytosis is thus more labile than exocytosis, perhaps due to the large number of proteins necessary for membrane fission (Koh et al. 2007). Therefore endocytosis rates reported here were evaluated as the mean of several trials per cell within the first 10 min after break-in, similar to other endocytosis protocols at this synapse (Yamashita et al. 2005).

We next determined that a change in membrane capacitance due to a 1-ms step depolarization to +10 or 0 mV is similar to that of a fiber-evoked AP at RT in young (P7–P10) and older (P16–P18) mouse calyx, respectively. Previous work has shown that the quantal content of an EPSC at the calyx

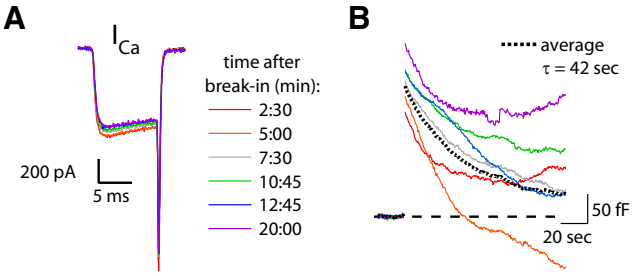

FIG. 1. Exocytosis and endocytosis are variable between trials. Sample recording of Ca^{2+} currents and resultant changes in membrane capacitance (C_m) from a P10 mouse calyceal terminal at room temperature (RT). *A*: Ca^{2+} currents recorded from a calyx of Held presynaptic terminal show minimal rundown over a 20-min period after break-in. Depolarizations were 10 ms in duration to 0 mV. *B*: exocytosis (ΔC_m jumps) and endocytosis (C_m decay) show significant intertrial variability, and endocytosis tends to run down after 15 min. Shown are single C_m sweeps of the same calyceal terminal as in *A* (color-matched to I_{Ca}). Endocytosis from this terminal is initially reliable, but tends to run down after 10–15 min after break-in. Resting C_m also showed an activity-independent drift and was 16.5 and 14 pF for this cell at the first and last sweeps shown, respectively. Average trace (dotted black line) is for the first 5 sweeps (from 0 to 12 min after break-in).

terminal is independent of temperature (Kushmerick et al. 2006). In young terminals (P7–P10), low-frequency stimulation at 0.1 Hz resulted in an average EPSC charge (area under the current waveform) of 17.1 ± 3.0 pC (n = 8) and an average quantal [miniature (m)EPSC] charge of 56.7 ± 5.1 fC (amplitude: 39.9 ± 4.1 pA) from the same cells (240 events per cell, on average). These values give an estimated quantal content (or exocytosis) of 310 ± 51 synaptic vesicles (SVs) per AP. Using an average capacitance of 61 aF per synaptic vesicle (Wu et al. 2007), this corresponds to a capacitance increase of 19.0 ± 3.1 fF for a single AP. In calyces from this age range, a step depolarization of 1 ms to +10 mV resulted in a capacitance increase of 23.3 ± 2.4 fF (n = 40). Depolarization of 1 ms to +10 mV also resulted in Ca^{2+} influx similar to that of previous studies, which estimated AP-equivalent stimulation parameters (Fedchyshyn and Wang 2005; Yang and Wang 2006). In P16–P18 animals, the average EPSC charge was 10.1 ± 1.8 pC (n = 11) and the average quantal (mEPSC) size charge from the same cells was 26.9 ± 2.4 fC (55.2 ± 3.1 pA, 123 events per cell, on average). This estimates a quantal content of 367 ± 44 quanta at RT, which corresponds to a capacitance increase of 22.4 ± 1.7 fF for a single AP, again assuming 61 aF per vesicle. Depolarization for 1 ms to 0 mV in older terminals (P14–P18) resulted in a capacitance increase of 33.5 ± 5.8 fF (n = 17). We thus considered a 1-ms depolarizing pulse as an approximately AP-like stimulus at the mouse calyx.

Endocytosis rate increases at physiological temperature

In about 80% of all calyces recorded from P7–P10 mice, membrane capacitance after the capacitance jump triggered by a depolarizing pulse decayed back toward baseline. This suggests the retrieval of fused vesicle membrane from the plasma membrane (Fig. 2, *A* and *B*). This decay could usually be accurately fit by a single or double exponential, and returned to baseline in most cases, although an overshoot beyond baseline membrane capacitance (C_m) was occasionally observed (Artalejo et al. 1995). Notably, capacitance decay (endocytosis) was seen only when we included 1 mM GTP in the intracellular solution (Yamashita et al. 2005). The rate of membrane retrieval occurred with a time constant of 10 to 50 s at RT and was linearly dependent on the magnitude of previous exocytosis for depolarizing pulses of 1 to 10 ms (Fig. 4*B*).

At PT, the rate of endocytosis sped up substantially both for short (AP-like) and longer (depleting) pulses, due to the addition of a second kinetically distinct exponential decay component (Fig. 2, *A* and *C*). This second component ($\tau \sim 1$ s) was roughly one order of magnitude faster than that seen at RT. The slower component of endocytosis at PT ($\tau \sim 20$–30 s) was similar to the rate seen at RT. A double-exponential function was thus necessary to produce a good fit of the C_m decay (see METHODS). The fast rate of endocytosis was responsible for 12–50% of the mean endocytosis over the stimulus durations examined. Specifically, for 1- to 5-ms depolarizations at PT, 9 of 20 terminals showed a fast component of decay, which accounted for about 30% of the total amplitude of C_m decay.

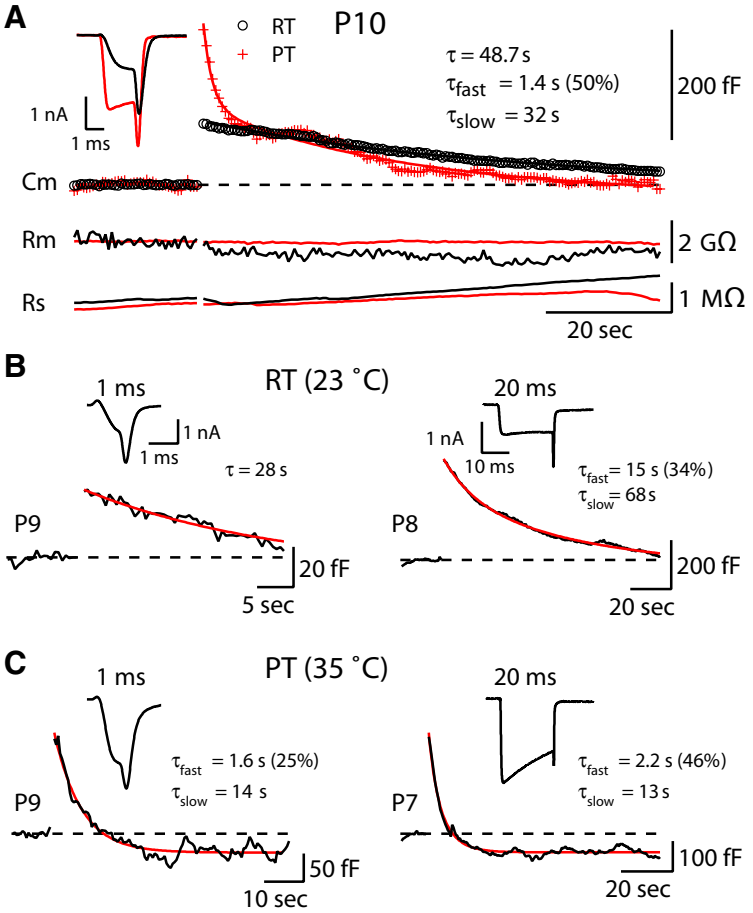

FIG. 2. A fast component of endocytosis appears at physiological temperature (PT). *A*: C_m of the calyx of Held terminal was monitored before and after a 2-ms depolarization to 0 mV. Depolarization at RT (black symbols) increased membrane capacitance by 110 fF, followed by a monoexponential return to baseline. When raised to PT, this same calyceal terminal responded to a 2-ms depolarization with a much larger capacitance jump (270 fF, red symbols), and endocytosis was fit by a double exponential composed of both fast and slow components. Average resting C_m for the cell shown was 18.6 pF at RT (7 sweeps) and 18.8 pF at PT (4 sweeps); average resting R_s was 1.4 MΩ at RT and 2 MΩ at PT; and average resting R_m was 9.3 GΩ at RT and 1.5 GΩ at PT. Ca^{2+} currents from the step depolarizations are shown in the *inset*. *B*: in young terminals at RT, examples of endocytosis after exocytosis are shown due to either a short pulse (1 to +10 ms) or a 20-ms depolarization to 0 mV. Endocytosis was relatively slow and well fit by a single or double exponential (red lines). Ca^{2+} currents are shown in the *inset*. Capacitance increased by 32 fF for the 1-ms depolarization and 396 fF for the 20-ms depolarization in these examples. Resting C_m was 18.5 pF for both terminals. *C*: at PT, a kinetically distinct fast component was added to endocytosis, for both short and long depolarizations. C_m decay was fit by a double exponential. Time constants (τ) of the fit and the relative contribution of the fast component are shown. Ca^{2+} currents are shown in the *inset*. Capacitance increased 162 fF for a 1-ms pulse and 293 fF due to a 20-ms depolarizing pulse in these terminals. Resting C_m was 31.5 and 15.6 pF, respectively.

By contrast, at RT, only 2 of 42 terminals showed a fast component of endocytosis for pulse durations of 1–10 ms.

One possible mechanism underlying the faster membrane retrieval rates seen at PT could be increased Ca^{2+} influx for a given depolarization duration, due to faster activation kinetics of Ca^{2+} channels at PT (Kushmerick et al. 2006). To test this hypothesis, we empirically matched Ca^{2+} influx at RT and PT, by reducing depolarization at PT to match the charge measured for a 2-ms depolarization at RT in the same cell (Fig. 3; $n = 6$ at RT, $n = 9$ at PT). Cells were recorded at RT, after which the temperature quickly ramped to PT ($n = 4$ terminals); or at PT first, after which the temperature decreased to RT ($n = 4$ terminals). When Ca^{2+} influx and exocytosis were matched at RT and PT, endocytosis was still significantly faster at PT, on average. Exponential fits to endocytosis from individual terminals resulted in mean time constants of 15.9 ± 2.6 s at RT ($n = 6$ terminals) and 8.0 ± 2.3 s for stimulus-matched terminals at PT ($n = 7$ terminals). This increase in endocytosis rate at PT was significant ($P = 0.045$, Student's t-test). Thus the faster endocytosis observed at PT for a short depolarizing voltage-clamp step is independent of Ca^{2+}-influx, indicating it is likely not due solely to a Ca^{2+}-dependent effect.

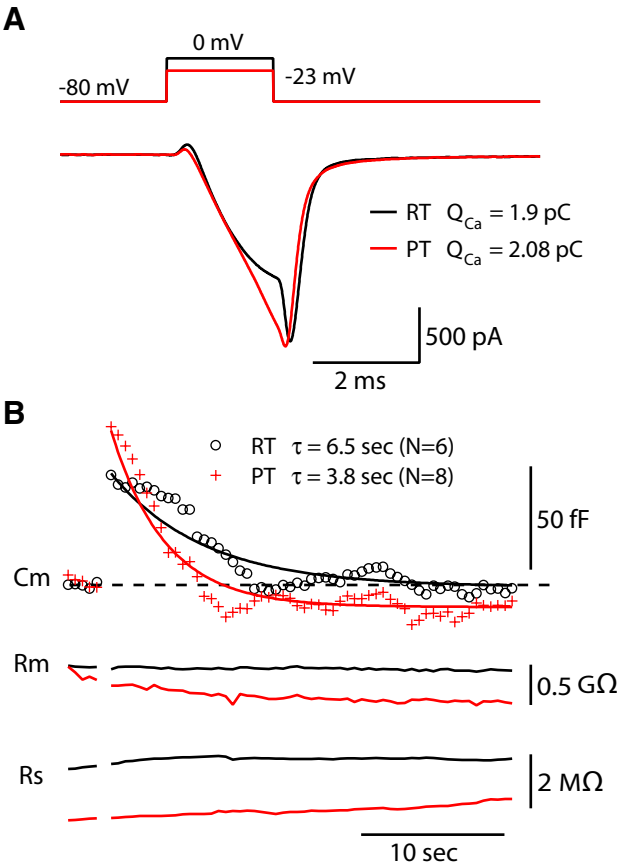

FIG. 3. Endocytosis rate at RT and PT with similar Ca^{2+} influx. *A*: a step depolarization (2 ms to 0 mV) in P7–P10 terminals at RT was matched at PT by reducing depolarization step from 0 mV to −23 mV, resulting in similar average Ca^{2+} influx (integral of the Ca^{2+} current: 1.9 ± 0.2 pC at RT; 2.1 ± 0.2 pC at PT; average currents from 6 terminals at RT and 9 terminals at PT; $P = 0.6$, Student's t-test). *B*: average capacitance measurements due to matched Ca^{2+} currents shown in *A* result in similar exocytosis (45.5 ± 5.8 fF at RT and 71.5 ± 13.0 fF at PT; $P = 0.16$, Student's t-test), but endocytosis was significantly accelerated almost twofold at PT. Average R_m was 1.8 ± 2.7 GΩ at RT and 1.7 ± 0.3 GΩ at PT. Average R_s was 17.2 ± 2.5 MΩ at RT and 15.3 ± 2.1 MΩ at PT. Values from each calyx terminal were the average of ≥3 individual sweeps (6 terminals at RT and 9 terminals at PT).

When mean endocytosis rate (τ_m) was plotted against the size of capacitance jump for 1- to 10-ms pulses, the data were fit well by a linear function (Fig. 4*B*). This result is consistent with previous reports (Sun et al. 2002; Yamashita et al. 2005). This slope, an exocytosis-dependent slowing of endocytosis rate, was not significantly different between RT and PT ($P = 0.5040$ Student's t-test), although overall rates were substantially faster. Even though the source of this endocytotic inhibition is still not clear, it may indicate a saturation of compensatory endocytotic ability of the terminal with increasing exocytosis.

At PT, the average endocytosis rate for 1-ms depolarizing pulses (AP-like) in immature terminals was $\tau = 7.6 \pm 2.2$ s ($n = 6$; Fig. 4*B*), which is significantly faster than that observed at RT [$\tau = 20.3 \pm 3.7$ s ($n = 25$); $P = 0.0064$ using Student's t-test corrected for unequal variances]. So the rate of endocytosis is more than twice as fast at PT than at RT, even though there is much more exocytosis at PT. Clearly, the ability to retrieve large amounts of vesicular membrane is greatly enhanced at PT.

Acceleration of endocytosis after prolonged depolarizations

For depolarizing steps >10 ms we observed an acceleration of endocytosis at RT (open symbols; Fig. 4*B*). For repetitive 20-ms depolarizations, recruitment of a Ca^{2+}-dependent, kinetically distinct form of fast endocytosis occurs in young rats at RT (Wu et al. 2005). We assume our results represent a similar Ca^{2+}-dependent acceleration of endocytosis due to strong stimulation, but now occurring at a lower threshold. We also observed a similar increase in endocytosis rate for depolarizations of 20 to 30 ms at PT in terminals of similar age animals, relative to the retrieval rates observed for 10-ms depolarization at PT (Fig. 4*B*). We assume that the mechanism underlying this acceleration in endocytosis rate is similar to that at RT.

Endocytosis capacity increases in mature synapses

Next, we investigated endocytosis in more mature synapses. Endocytosis rates for young and mature terminals were similar in response to a 1-ms depolarization (Fig. 5, *A* and *B*). Mature calyces had $\tau = 14.5 \pm 3.6$ s ($n = 5$) and endocytosis in immature calyces had $\tau = 20.3 \pm 3.7$ s ($n = 25$; $P = 0.4992$, Student's t-test). However, the amount of exocytosis increased dramatically in older animals (Fig. 7*A*), especially for short depolarizations, due to an increased pool size and more efficient excitation–secretion coupling in older animals (Fedchyshyn and Wang 2005; Taschenberger et al. 2002).

We depolarized the terminal in older animals over a variety of durations (1–30 ms) at RT and noticed a clear lack of dependence of endocytosis rate on the magnitude of ΔC_m or exocytosis (Figs. 5*B* and 7). In more mature calyces, endocytosis was fit almost exclusively by a single exponential at RT. Biexponential endocytosis was seen in one of six cells at 5 ms (contributing to 50% of mean endocytosis in that calyx) and one of five cells at 30 ms (contributing 50% of mean endocytosis in that calyx). Across the depolarization range examined here, the rate of endocytosis had a time constant of $\tau = 16$ s,

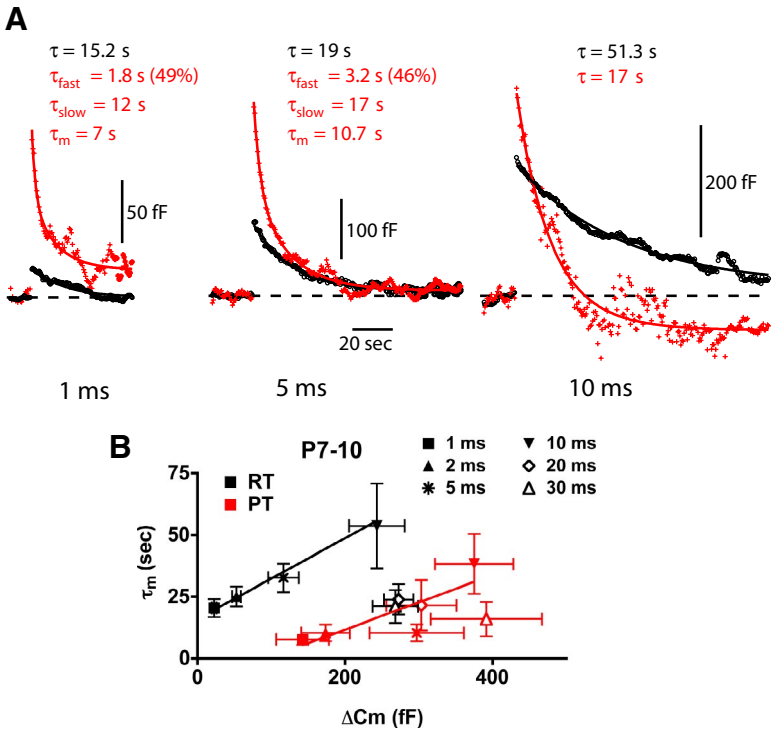

FIG. 4. Endocytosis and exocytosis coupling at RT and PT. Summary data for membrane capacitance decay (endocytosis) in P7–P10 calyces at RT (black) and PT (red) at a variety of depolarizing pulse durations. *A*: PT dramatically increases exocytosis, especially for shorter-duration pulses (1–5 ms) relative to RT. Rate of endocytosis speeds up at PT and becomes better estimated by a double-exponential function, with a significant fraction occurring in the first 10 s after depolarization. Timescale is shared for all 3 panels in *A*. *B*: rate of endocytosis is proportional to exocytosis in immature calyces for pulses of 1 to 10 ms. Mean endocytosis rate (weighted time constant τ_m; see METHODS) was plotted against mean capacitance jump due to depolarizing pulses of 1- to 30-ms duration. For 1–10 ms pulses at RT or PT (closed symbols), a straight line fits the data well (slope = 164.1 ± 46.8 ms/fF for RT; slope = 110.6 ± 35.9 ms/fF for PT). For step depolarizations >10 ms, the mean endocytosis rate at RT accelerated to rates similar to that seen at PT (open symbols). At RT, n = 25 calyx terminals for 1 ms, n = 21 for 2-ms, n = 7 for 5-ms, n = 5 for 10-ms, n = 21 for 20-ms, and n = 6 for 30-ms depolarizations. At PT, n = 6 terminals for 1- and 2-ms, and n = 5 for 5-, 10-, 20-, and 30-ms depolarizations.

regardless of the magnitude of exocytosis or depolarizing pulse duration.

Evaluation of endocytotic capacity in terms of maximum retrieval rates immediately after depolarization [synaptic vesicles per second (SV/s)] shows that the capacity for vesicle retrieval increases in older calyceal terminals proportionally to exocytosis, and does not saturate. For a 1-ms depolarization (τ_m = 14.5 s), maximum retrieval rate at RT for older terminals can be approximated as $\Delta C_m/\tau_m/(C_m/\text{vesicle})$ = 68.1 fF/14.51 s/0.061 fF/SV = 77 SV/s. For a 30-ms depolarization, the maximum retrieval rate increases to 534 SV/s, whereas the time constant for endocytosis stays nearly constant (τ = 15.7 s). We thus propose that mature synapses have a greater capacity to retrieve membrane due to a more abundant set of endocytotic proteins and/or efficient endocytotic machinery. A developmental increase in the number of retrieval sites or development of a stronger interaction between the endocytotic machinery and newly exocytosed vesicles could both be responsible.

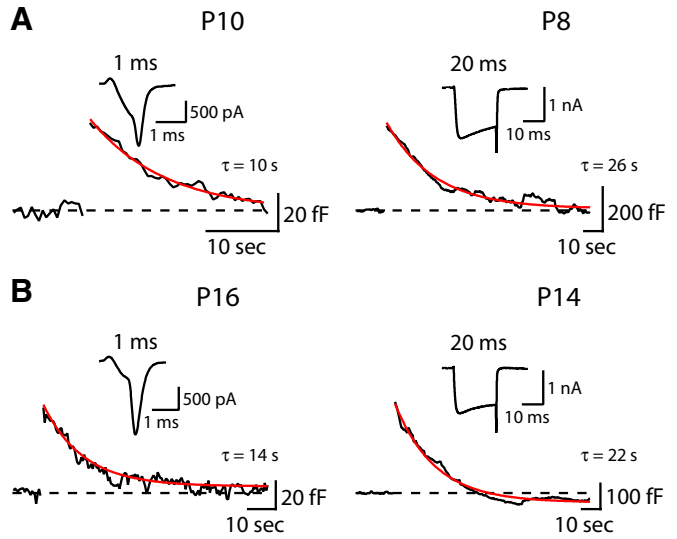

FIG. 5. Monoexponential time course for endocytosis in calyx terminals at RT during development. *A*: examples of immature terminals that show a rate of endocytosis that was well fit by a single exponential (red line). A 1-ms depolarization resulted in a capacitance increase of 45 fF (*left*). Longer depolarization (20 ms, *right*) gave rise to a much larger capacitance jump (365 fF) but similar capacitance decay. Resting C_m for the cells shown are 19.4 pF (*left*) and 17.4 pF (*right*). *B*: examples of more mature terminals (P14–P16), where a 1-ms depolarization resulted in a capacitance jump (55 fF; *left*), that decayed with the time course of a single exponential. Longer depolarization (20 ms) induced larger exocytosis (360 fF), but similar rates of endocytosis, which were fit by a monoexponential function. Resting C_m for the cells shown here are 18 pF (*left*) and 12.9 pF (*right*).

We also directly measured endocytosis rates in older terminals at PT for depolarization lengths of 2 and 30 ms, to estimate the maximum vesicle retrieval rate immediately after exocytosis in mature functional terminals at PT (Fig. 6). Capacitance decay in these recordings was very fast and returned to baseline within 20 s. Data from calyx terminals for 2-ms pulses were well fit by a single-exponential function (τ = 3.3 ± 0.8 s, n = 6 for 2-ms depolarization). For 30-ms depolarizations, τ_m = 7.6 ± 2.8 s, with two of four terminals returning a biexponential fit. For these two terminals, τ_{fast} = 2.3 ± 0.3 s, carrying 66 ± 1% of the total time constant, and τ_{slow} = 31.5 ± 6.3 s. Thus at PT maximum retrieval rates can be estimated as 921 and 1,045 SV/s, for a 2- and 30-ms depolarization, respectively. We measured the quantal content of an evoked EPSC as about 295 SV in P16–P18 mice at PT (n = 5 terminals; data not shown). This result suggests that the mature calyx could operate indefinitely at frequencies of approximately 3.3 Hz without depression, solely by local recycling of SV membrane. Because this calyx synapse can actually follow much higher stimulation frequencies, we propose that it additionally taps into a large reserve pool of vesicles to support sustained high-frequency synaptic transmission at PT.

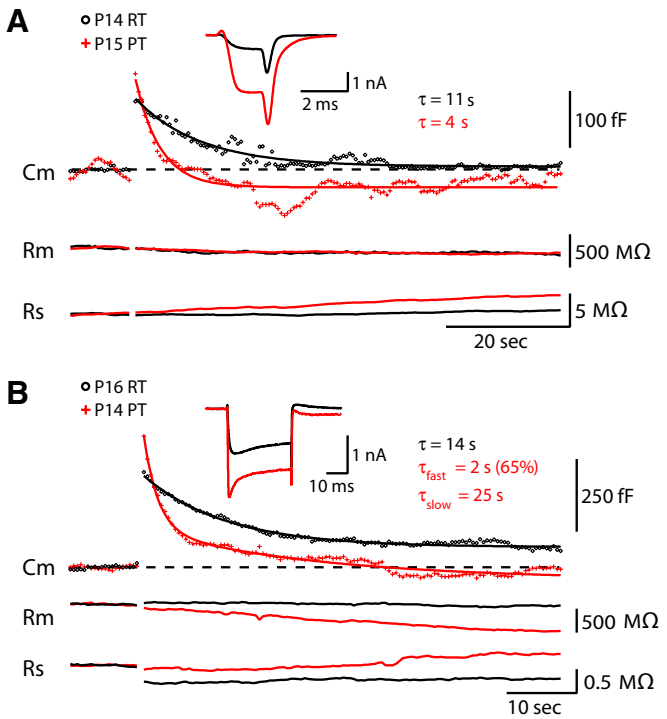

FIG. 6. Endocytosis in more mature terminals speeds up at PT. Sample traces from P14–P16 terminals recorded at RT or PT. *A*: short 2-ms depolarizations resulted in a capacitance jump of 114 fF at RT (*black traces*; P14 animal, resting C_m = 14.1 pF). At PT (*red traces*), a 2-ms depolarization resulted in a jump of 202 fF (P15 animal, resting C_m = 18.4 pF). Endocytosis was fit by a monoexponential function both at RT and PT. *Inset*: respective Ca^{2+} currents. *B*: longer 30-ms depolarization resulted in jumps of 294 fF at RT (P16 animal, resting C_m = 11.1 pF), and 446 fF at PT (P14 animal, resting C_m = 19.9 pF). Endocytosis was fit by a monoexponential function at RT, but required a biexponential fit function at PT. Weighted time constant (τ_m) for endocytosis due to a 30-ms jump at PT was 10.1 s (see METHODS). *Inset*: respective Ca^{2+} currents. Ca^{2+} current inactivation was fit by a monoexponential function at RT (τ = 15 ms) and a biexponential function at PT (τ_{fast} = 2.2 ms, carrying 59% of the decay; τ_{slow} = 18.6 ms; and τ_m = 8.9 ms).

Ca^{2+}-dependent acceleration of endocytosis is developmentally regulated

To investigate further the Ca^{2+} dependence of endocytosis, we plotted the endocytotic rate constant against Ca^{2+} charge influx elicited by depolarization (Fig. 8). As expected, a curve similar to that for exocytosis versus endocytosis was generated. For similar Ca^{2+} charge (Q_{Ca}) influxes produced by short depolarizations (AP-like), endocytosis at PT was significantly faster than that at RT: Q_{Ca} for 1-ms at PT was similar to that for 2-ms depolarization at RT (1.9 ± 0.4 pC for 1 ms at PT, n = 6; 1.9 ± 0.1 pC for 2 ms at RT, n = 18; P = 0.9388 by Student's *t*-test); however, endocytosis was significantly faster at PT (τ = 7.6 ± 2.3 s at PT; 25.0 ± 4.1 s at RT; P = 0.0132 by Mann–Whitney nonparametric *U* test). A similar trend was seen when 2-ms depolarization at PT was compared with 5-ms depolarization at RT (Q_{Ca} = 3.9 ± 0.4 pC for 2 ms at PT, n = 5; 5.1 ± 0.6 pC for 5 ms at RT, n = 7; P = 0.1473), with faster endocytosis at PT (τ = 11.3 ± 3.0 s at PT and 32.6 ±5.7 s for RT; P = 0.0041 by Mann–Whitney *U* test). Likewise, comparing 5 ms at PT to 10 ms at RT yielded similar Q_{Ca} (10.0 ± 2.9 pC for 5 ms at PT, n = 4; 12.6 ± 2.2 pC for 10 ms at RT, n = 5; P = 0.5343), but significantly faster endocytosis at PT (τ = 10.3 ± 3.4 s at PT and 53.6 ± 17.2 s at RT; P = 0.0159 by Mann–Whitney *U* test). These results further support the premise that endocytosis at PT is not faster strictly due to increased Ca^{2+} influx.

Endocytosis due to longer depolarizations was accelerated in a Ca^{2+}-dependent manner in younger terminals, both at RT and PT. In younger animals, endocytosis was slowest for a 10-ms depolarization, both at RT and PT (Fig. 8*A*). For 20- and 30-ms pulses at either RT or PT, endocytosis accelerated to rates similar to those observed for brief stimuli (Fig. 4, *A* and *B*). We assume that this result indicates a "threshold" for Ca^{2+}-dependent acceleration of endocytosis at about 10–12 pC Ca^{2+} influx in the immature calyx of Held terminal (see also Wu et al. 2005).

A Ca^{2+}-dependent acceleration of endocytosis for 20- to 30-ms pulses was not present in more mature terminals (P14–P18), where endocytosis was well represented by similar monoexponential rates for both short and long depolarizations (Fig. 8*B*). These data can be fit by a linear function (slope = 66.4 ± 151.2 ms/pC). At RT, Ca^{2+} influx was similar at P7–P10 and P14–P18 terminals at 5- and 10-ms depolarizations, but endocytosis was faster in older terminals. For 5-ms depolarization, Q_{Ca} was not significantly different (5.0 ± 0.6 pC for P7–P10, n = 7; 8.2 ± 1.7 pC for P14–P18, n = 6; P = 0.0632), but the endocytosis rate was significantly faster in older terminals (τ = 32.6 ± 5.7 s for P7–P10 and 12.2 ± 1.9 s for P14–P18; P = 0.0082 by Mann–Whitney *U* test). For a 10-ms depolarization, similar Q_{Ca} values were observed (12.6 ± 2.2 pC for P7–P10, n = 5; 14.6 ± 1.5 pC for P14–P18, n = 7; P = 0.4755), although the endocytosis rate was also significantly faster in P14–P18 terminals (τ = 53.6 ± 17.2 s for P7–P10 and τ = 14.3 ± 3.1 s for P14–P18; P = 0.0177, Mann–Whitney *U* test). This surprising lack of slowing of endocytosis in older animals may be due to an increased accumulation of endocytotic proteins and/or sites.

We thus suggest that the endocytotic machinery in older animals is not saturated even when a majority of the synaptic vesicles in the readily releasable pool are exocytosed (vesicle pool depletion), perhaps due to a larger supply of active endocytotic sites. Although the exact mechanism remains unclear, the mature terminal seems capable of supporting an increased releasable pool size and an increased rate of pool refilling in older animals (Kushmerick et al. 2006), perhaps in part due to this increased capacity for sustained endocytosis.

DISCUSSION

We used membrane capacitance measurements to directly assay the rate of endocytosis of the calyx of Held terminal at RT and PT in young mice. We also examined the speed of endocytosis in older mice (P14–P18) when the calyx is more functionally mature. Increasing the amount of exocytosis slows down endocytosis at RT in immature animals, consistent with previous reports for pulse durations <10 ms (Sun et al. 2002; Yamashita et al. 2005). However, we find that for longer depolarizing pulses (20–30 ms) endocytosis accelerates. At PT, the endocytosis rate is augmented by a second, faster rate, which is responsible for about 25% of the mean endocytosis time constant in the young calyx, and closer to 67% in older terminals. Additionally, in older animals the endocytotic rate was independent of stimulation intensity (or depolarizing pulse duration). The capacity to quickly endocytose relatively large

amounts of exocytosed membrane is thus substantially enhanced in more mature synapses.

Exocytosis and endocytosis in young calyces at RT

Previous reports showed a linear dependence of endocytosis rate on capacitance jump (exocytosis) for depolarizing steps ≤10 ms (Yamashita et al. 2005). Surprisingly, when we fully exhausted the readily releasable pool in young animals at RT (depolarization >10 ms), the rate of endocytosis increased. Recently, it has been shown that endocytosis speeds up after prolonged stimulation trains in a Ca^{2+}-dependent manner (Wu et al. 2005), and $[Ca^{2+}]_i$ and calmodulin accelerate the refilling of a fast releasable pool (Sakaba and Neher 2001a; Wang and Kaczmarek 1998). A 20- to 30-ms stimulation may induce the release of a reluctant pool of vesicles, which are then preferentially retrieved by a fast pathway. Heterogeneity in the releasable pool at the calyx of Held was previously shown to consist of a quickly releasing pool of vesicles, which are slowly recycled, and a slowly releasing pool that is quickly refilled (Sakaba 2006; Sakaba and Neher 2001a; Trommershauser et al. 2003). Refilling of quickly releasable vesicles is modulated by cAMP and calmodulin (Sakaba and Neher 2001a,b). The identities of these pools may be linked to differential sensitivity to Ca^{2+}, to submaximal release rates, or to distance to Ca^{2+} sources (Wadel et al. 2007; Wolfel et al. 2007). It is possible that these differences are conveyed to vesicle retrieval rates, as well.

What is the source of the synaptic vesicles responsible for refilling the releasable vesicle pool at the calyx of Held? Postsynaptic studies in immature rats (P8–P10) at RT have shown that recovery from synaptic depression is frequency dependent. Moderate stimulation (10–100 Hz) recovers with a τ = 4 s (von Gersdorff et al. 1997), whereas strong stimulation (300 Hz) invokes two phases of recovery: fast recovery (τ <100 ms) and a slower form (τ = 4–5 s; Wang and Kaczmarek 1998). Furthermore, refilling of the vesicle pool requires polymerized actin (Sakaba and Neher 2003), and presynaptic inhibition of dynamin abolishes endocytosis and eventually inhibits exocytosis (Yamashita et al. 2005). These results indicate that reuse of synaptic vesicles is partially responsible for the refilling of the pool. Moreover, studies using lipophilic dyes to label recycling of vesicles have shown that with rather low frequency stimulation, only a subset of vesicles is used (de Lange et al. 2003). However, these studies cannot fully discriminate between partial replenishment of the releasable pool from intracellular reserves, or immediate refilling and reuse of recently fused vesicles. Our results support the conclusion that local vesicle recycling plays an important role in the maintenance of fusion-competent synaptic vesicles and helps to determine the possible maximal rates of local reuse of vesicles at the calyx of Held, under immature and more mature conditions, and at physiological temperatures.

The adult calyx of Held is capable of entrained synaptic transmission at 600 Hz in mature mouse terminals for short periods of afferent fiber stimulation (Wu and Kelly 1993). However, we estimate that the maximal rate of transmission, based solely on local vesicle reuse, is only about 3 Hz at PT in terminals from P16–P18 animals. This apparent discrepancy requires clarification. Although the calyceal terminal is capable of following high stimulation frequencies, it is not capable of doing so indefinitely, and undergoes substantial depression, even at relatively low frequencies (e.g., 10 to 100 Hz; von Gersdorff and Borst 2002). At stimulation frequencies >100 Hz at RT, depression seems to be mediated principally by vesicle pool depletion. We thus propose that the calyx of Held relies on a ready supply of vesicles from a reserve pool to follow higher stimulation frequencies.

Unfortunately, we cannot fully account for the fate of excess synaptic vesicle membrane during high-frequency stimulation. Bulk endocytosis has been shown at other large presynaptic terminals (Holt et al. 2003; LoGiudice and Matthews 2007). There is also evidence of bulk endocytosis at the calyx of Held, although its relative contribution (10% of all endocytosis) probably does not fully account for the complete retrieval of exocytosed membrane after strong stimulation (Wu and Wu 2007).

What does faster endocytosis at PT reflect?

At the calyx of Held, Ca^{2+} channel activation and recovery from short-term depression are faster at PT, and the recruitment of vesicles during steady-state synaptic depression is also accelerated at PT, whereas initial vesicle pool size and excitation–secretion coupling are relatively unaffected (Kushmerick et al. 2006; Postlethwaite et al. 2007). Here we saw a significant increase in the mean endocytosis rate at PT, due to the addition of a kinetically distinct fast form of endocytosis. Two previous studies also examined the effect of temperature on vesicle retrieval in neuronal presynaptic terminals, using optical methods, and reported an increase in the speed of endocytosis. In hippocampal cultured synapses, Fernandez-Alfonso and Ryan (2004) reported a Q_{10} for endocytosis of 1.4, allowing endocytosis to sustain vesicle exocytosis at PT for stimulation frequencies ≤10 Hz (i.e., a frequency that would normally deplete the releasable pool at RT); and Micheva and Smith (2005) estimated that the endocytosis rate increases threefold at PT. Here we observed an average 1.44-fold faster endocytosis at PT (for a 12°C increase). This faster endocytosis at PT is compelling but still circumstantial evidence that the retrieval of vesicle membrane may be a rate-limiting factor for continued high-frequency transmission at room temperature (von Gersdorff and Borst 2002).

This fast component of endocytosis at PT could reflect the preferential activation of a modulatory pathway, or an increase in the rate of clathrin-mediated endocytosis, or the addition of a distinct temperature-sensitive mechanism not seen at RT. Alternatively, an additional, faster component of endocytosis may be activated at PT simply due to increased enzymatic activity of GTPases involved in membrane fission and/or increased ease of vesicle budding from the cell membrane due to increased fluidity of the lipid membrane.

Increased intraterminal Ca^{2+}, due to either prolonged depolarization or ionophore application, has been shown to facilitate endocytosis at RT (Teng and Wilkinson 2005; Wu et al. 2005) and could represent a pathway that may be activated at lower threshold at PT. Although Ca^{2+} influx is significantly increased at PT, especially for short pulses (Kushmerick et al. 2006), we show here that the temperature-dependent effect seems to be independent of Ca^{2+} influx or depolarization length (Figs. 3 and 8*A*). In addition, we note that the rate of Ca^{2+} extrusion is dramatically increased at PT (Helmchen

et al. 1997; Kimura et al. 1987). Thus we propose that the increased endocytosis rate at PT is not due to activation of an additional Ca^{2+}-dependent endocytotic pathway.

Studies at the vertebrate neuromuscular junction support the hypothesis that the increase in endocytotic rate at PT is due to a speeding of the clathrin-mediated mode of retrieval (Teng and Wilkinson 2000). These studies show that the uncoating of clathrin from retrieved vesicles after endocytosis is strongly temperature dependent and may be a rate-limiting step for ≤50% of endocytosis after prolonged stimulation (Teng and Wilkinson 2000). The activity of clathrin-mediated endocytotic proteins (e.g., auxilin, synaptojanin, endophilin) may thus be rate limiting for endocytosis at RT (Jung and Haucke 2007). We thus suggest that an increased activity of proteins that catalyze endocytosis, specifically the fission reaction measured here using C_m measurements, may be responsible for the faster endocytosis rates observed at PT.

The fast endocytosis we observe at PT could alternatively represent rapid nonclathrin-mediated endocytosis (e.g., "kiss and run" exo-endocytosis à la Ceccarelli et al. 1973). Indeed, the existence of this fast form of exo-endocytosis has recently been shown to occur for a small subset (~5%) of single vesicle events at the calyx of Held at RT (He et al. 2006). It is therefore possible that PT increases the contribution of fast clathrin-independent endocytosis to a detectable level using whole cell capacitance measurements.

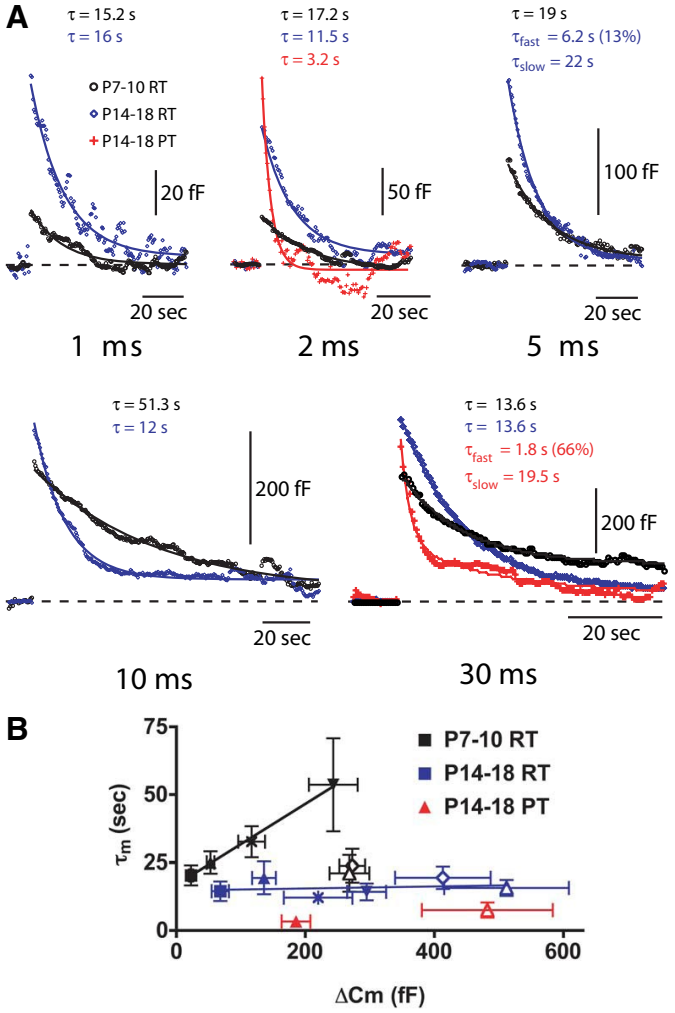

FIG. 7. Synaptic maturation increases the capacity for endocytosis. Compared with immature calyces, endocytosis is faster in more mature calyces for a given depolarizing pulse, even though ΔC_m jumps are substantially larger for more mature terminals. *A*: summary capacitance decay data for 1- to 30-ms depolarizations are shown for immature terminals at RT (P7–P10; *black traces*), for mature terminals at RT (P14–P18; *blue traces*), and mature terminals at PT (P14–P18; *red traces*). n = 4–25 calyx terminals for each depolarization length. *B*: in mature calyces, the mean endocytosis rate vs. exocytosis at RT was fit by a line with a slope that was not significantly different from zero (3.8 ± 10.1 ms/fF) for step depolarizations of 1–30 ms in duration. n = 5 terminals for 1- and 2-ms, n = 6 for 5-ms, n = 7 for 10-ms, n = 6 for 20-ms, and n = 5 for 30-ms depolarization at RT. For mature terminals at PT, endocytosis was faster than that at RT for both short and longer depolarizations (n = 6 for 2-ms, n = 4 for 30-ms depolarization). Data for P7–P10 terminals at RT is the same as in Fig. 4.

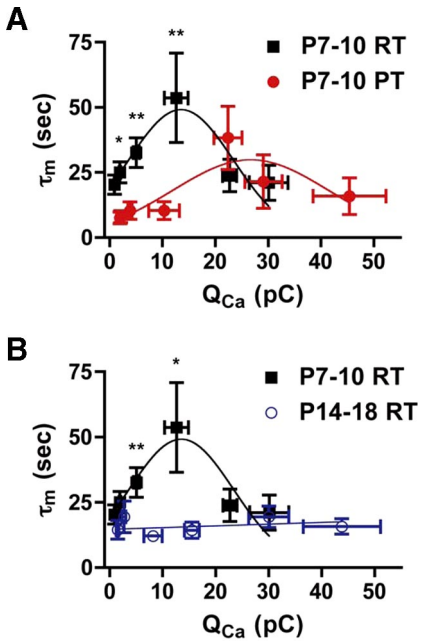

FIG. 8. Endocytosis: dependence on Ca influx, temperature, and age. *A*: plotting the mean endocytosis rate against calcium influx illustrates the Ca^{2+} dependence of endocytosis in younger animals. Endocytosis rate was slowest at around 10-ms depolarization at RT (black symbols). At PT (red symbols), endocytosis was similarly slowed at 10-ms depolarization, although Q_{Ca} (integral of I_{Ca}) was larger and endocytosis rate was faster. Lines are Gaussian fits to the data used to guide the eye. For similar Q_{Ca}, endocytosis at PT was significantly faster than that at RT, as indicated by the asterisks. *B*: endocytosis rate showed no significant dependence on Ca^{2+} influx in mature terminals (blue open symbols), and was faster at all depolarizations examined (1- to 30-ms pulses). Endocytosis in older animals was significantly faster than that for immature terminals at 5 and 10 ms, although Q_{Ca} was similar at these depolarizing pulse durations.

Endocytotic rates in more mature nerve terminals

We observed a constant endocytosis rate over a wide range of depolarizing pulse durations in calyces from older animals at RT (Fig. 7 and 8*B*). This differs greatly from what has been observed in younger animals (Fig. 7*B*; Sun et al. 2002; Yamashita et al. 2005). Moreover, the average time constant we observed ($\tau \approx 15$ s) is nearly identical to that recently reported for hippocampal synapses using optical imaging methods (Granseth et al. 2006). It is possible that the "threshold" for a Ca^{2+}-dependent acceleration of endocytosis is lower in older animals (Gad et al. 1998), or more closely coupled to Ca^{2+}

influx, analogous to developmental changes seen for excitation–secretion coupling at the calyx (Fedchyshyn and Wang 2005). Interestingly, dynamin expression levels increase during postnatal synaptic maturation (Cnops et al. 2007). Development also induces the expression of a calcineurin-dependent form of endocytosis in isolated cortical synapses, 2–4 wk after birth (Smillie et al. 2005). A similar effect could be present at the calyx of Held, although we found no effect of the calcineurin inhibitor cypermethrin (200 nM to 2 μM) on endocytosis in P16 terminals (data not shown). We also note that intraterminal Ca^{2+} is extruded faster from older calyces (Chuhma and Ohmori 2001). Thus $[Ca^{2+}]_i$ changes may be more tightly regulated in older calyces (Felmy and Schneggenburger 2004).

If endocytosis is no longer saturating in older animals, this may indicate that endocytosis hotspots increase supralinearly to the number of active zones during maturation. A 30-ms depolarization resulted in a capacitance jump of 510 fF in older animals at RT (Fig. 6*B*), which on average represents the exocytosis of about 8,000 synaptic vesicles (SVs). There are only about 600 active zones (AZs) in the P14 rat calyx (Taschenberger et al. 2002), but the retrieval rate in older terminals varies from 77 to 534 SV/s, showing no apparent saturation, even for a depolarizing pulse that probably depletes the releasable pool of synaptic vesicles.

Endocytotic proteins, and presumably sites for vesicle retrieval, are localized near—but separate from—active zones within other large presynaptic terminals (Fergestad and Broadie 2001; Koh et al. 2007; Roos and Kelly 1999; Teng et al. 1999). Although the number of AZs in the calyx remains similar between the two ages studied here (500 AZs at P9; Satzler et al. 2002; Taschenberger et al. 2002), apparently there is substantial refinement in the mechanisms underlying synaptic vesicle retrieval. If we assume that the capacitance of individual SVs and the retrieval rate per site remain constant during development, then an apparent increase in endocytotic capacity predicts a dramatic increase in endocytotic hot spots in older animals, 36-fold between P7–P10 and P14–P18 (from 0.2 to 7.2 $SV \cdot s^{-1} \cdot AZ^{-1}$; see METHODS). Interestingly, the rate of endocytosis we report for mature calyces at RT is roughly similar to that seen at the mossy fiber bouton of rats at a similar age, around 4 $SV \cdot s^{-1} \cdot AZ^{-1}$ (Hallermann et al. 2003). Concomitant increases in the number of endocytotic sites, and thus the capacity for endocytosis, and reducing the probability for synaptic vesicle release at AZs (Taschenberger et al. 2002) would increase the capacity of this more mature synapse for sustained high-frequency activity.

In conclusion, we find that akin to other aspects of the synaptic vesicle cycle, the rate of endocytosis at the calyx of Held changes dramatically at physiological temperature and over the course of postnatal development. Our findings suggest that the calyx acquires a substantial capacity for fast and complete membrane retrieval following copious exocytosis after the onset of hearing. This likely adds further to its ability to sustain high-frequency transmission for prolonged periods, as suggested by in vivo recordings from more mature animals (Guinan and Li 1990) and by in vitro recordings after a period of extended synaptic rest or inactivity (Hermann et al. 2007).

ACKNOWLEDGMENTS

We thank Dr. Christopher Kushmerick (Universidade Federal de Minas Gerais, Belo Horizonte, Brazil) for helpful comments and discussions.

GRANTS

This work was supported partly by a National Institute of Deafness and Communication Disorders (NIDCD) National Research Service Award Fellowship DCD-06768 to R. Renden and grants from the Human Frontier Science Program and NIDCD to H. von Gersdorff.

REFERENCES

Aravanis AM, Pyle JL, Tsien RW. Single synaptic vesicles fusing transiently and successively without loss of identity. *Nature* 423: 643–647, 2003.

Artalejo CR, Henley JR, McNiven MA, Palfrey HC. Rapid endocytosis coupled to exocytosis in adrenal chromaffin cells involves Ca^{2+}, GTP, and dynamin but not clathrin. *Proc Natl Acad Sci USA* 92: 8328–8332, 1995.

Betz WJ, Angleson JK. The synaptic vesicle cycle. *Annu Rev Physiol* 60: 347–363, 1998.

Blatchley BJ, Cooper WA, Coleman JR. Development of auditory brainstem response to tone pip stimuli in the rat. *Brain Res* 429: 75–84, 1987.

Borst JG, Helmchen F, Sakmann B. Pre- and postsynaptic whole-cell recordings in the medial nucleus of the trapezoid body of the rat. *J Physiol* 489: 825–840, 1995.

Ceccarelli B, Hurlbut WP, Mauro A. Turnover of transmitter and synaptic vesicles at the frog neuromuscular junction. *J Cell Biol* 57: 499–524, 1973.

Chuhma N, Ohmori H. Differential development of Ca^{2+} dynamics in presynaptic terminal and postsynaptic neuron of the rat auditory synapse. *Brain Res* 904: 341–344, 2001.

Cnops L, Hu TT, Vanden Broeck J, Burnat K, van den Bergh G, Arckens L. Age- and experience-dependent expression of dynamin I and synaptotagmin I in cat visual system. *J Comp Neurol* 504: 254–264, 2007.

de Lange RP, de Roos AD, Borst JG. Two modes of vesicle recycling in the rat calyx of Held. *J Neurosci* 23: 10164–10173, 2003.

Fedchyshyn MJ, Wang LY. Developmental transformation of the release modality at the calyx of Held synapse. *J Neurosci* 25: 4131–4140, 2005.

Felmy F, Schneggenburger R. Developmental expression of the Ca^{2+}-binding proteins calretinin and parvalbumin at the calyx of Held of rats and mice. *Eur J Neurosci* 20: 1473–1482, 2004.

Fergestad T, Broadie K. Interaction of stoned and synaptotagmin in synaptic vesicle endocytosis. *J Neurosci* 21: 1218–1227, 2001.

Ferguson SM, Brasnjo G, Hayashi M, Wolfel M, Collesi C, Giovedi S, Raimondi A, Gong LW, Ariel P, Paradise S, O'Toole E, Flavell R, Cremona O, Miesenbock G, Ryan TA, De Camilli P. A selective activity-dependent requirement for dynamin 1 in synaptic vesicle endocytosis. *Science* 316: 570–574, 2007.

Fernandez-Alfonso T, Ryan TA. The kinetics of synaptic vesicle pool depletion at CNS synaptic terminals. *Neuron* 41: 943–953, 2004.

Forsythe ID. Direct patch recording from identified presynaptic terminals mediating glutamatergic EPSCs in the rat CNS, in vitro. *J Physiol* 479: 381–387, 1994.

Gad H, Low P, Zotova E, Brodin L, Shupliakov O. Dissociation between Ca^{2+}-triggered synaptic vesicle exocytosis and clathrin-mediated endocytosis at a central synapse. *Neuron* 21: 607–616, 1998.

Gandhi SP, Stevens CF. Three modes of synaptic vesicular recycling revealed by single-vesicle imaging. *Nature* 423: 607–613, 2003.

Gillis KD. Techniques for membrane capacitance measurements. In: *Single-Channel Recording* (2nd ed.), edited by Sakmann B, Neher E. New York: Plenum Press, 1995, p. 155–198.

Granseth B, Odermatt B, Royle SJ, Lagnado L. Clathrin-mediated endocytosis is the dominant mechanism of vesicle retrieval at hippocampal synapses. *Neuron* 51: 773–786, 2006.

Guinan JJ Jr, Li RY. Signal processing in brainstem auditory neurons which receive giant endings (calyces of Held) in the medial nucleus of the trapezoid body of the cat. *Hear Res* 49: 321–334, 1990.

Hallermann S, Pawlu C, Jonas P, Heckmann M. A large pool of releasable vesicles in a cortical glutamatergic synapse. *Proc Natl Acad Sci USA* 100: 8975–8980, 2003.

He L, Wu XS, Mohan R, Wu LG. Two modes of fusion pore opening revealed by cell-attached recordings at a synapse. *Nature* 444: 102–105, 2006.

Heidelberger R, Zhou ZY, Matthews G. Multiple components of membrane retrieval in synaptic terminals revealed by changes in hydrostatic pressure. *J Neurophysiol* 88: 2509–2517, 2002.

Helmchen F, Borst JG, Sakmann B. Calcium dynamics associated with a single action potential in a CNS presynaptic terminal. *Biophys J* 72: 1458–1471, 1997.

Hermann J, Pecka M, von Gersdorff H, Grothe B, Klug A. Synaptic transmission at the calyx of Held under in vivo like activity levels. *J Neurophysiol* 98: 807–820, 2007.

Holt M, Cooke A, Wu MM, Lagnado L. Bulk membrane retrieval in the synaptic terminal of retinal bipolar cells. *J Neurosci* 23: 1329–1339, 2003.

Horrigan FT, Bookman RJ. Releasable pools and the kinetics of exocytosis in adrenal chromaffin cells. *Neuron* 13: 1119–1129, 1994.

Hull C, von Gersdorff H. Fast endocytosis is inhibited by GABA-mediated chloride influx at a presynaptic terminal. *Neuron* 44: 469–482, 2004.

Johnson SL, Marcotti W, Kros CJ. Increase in efficiency and reduction in Ca^{2+} dependence of exocytosis during development of mouse inner hair cells. *J Physiol* 563: 177–191, 2005.

Jung N, Haucke V. Clathrin-mediated endocytosis at synapses. *Traffic* 8: 1129–1136, 2007.

Kimura J, Miyamae S, Noma A. Identification of sodium-calcium exchange current in single ventricular cells of guinea-pig. *J Physiol* 384: 199–222, 1987.

Koh T-W, Korolchuk VI, Wairkar YP, Jiao W, Evergren E, Pan H, Zhou Y, Venken KJT, Shupliakov O, Robinson IM, O'Kane CJ, Bellen HJ. Eps15 and Dap160 control synaptic vesicle membrane retrieval and synapse development. *J Cell Biol* 178: 309–322, 2007.

Kushmerick C, Renden R, von Gersdorff H. Physiological temperatures reduce the rate of vesicle pool depletion and short-term depression via an acceleration of vesicle recruitment. *J Neurosci* 26: 1366–1377, 2006.

LoGiudice L, Matthews G. Endocytosis at ribbon synapses. *Traffic* 8: 1123–1128, 2007.

Micheva KD, Smith SJ. Strong effects of subphysiological temperature on the function and plasticity of mammalian presynaptic terminals. *J Neurosci* 25: 7481–7488, 2005.

Moser T, Beutner D. Kinetics of exocytosis and endocytosis at the cochlear inner hair cell afferent synapse of the mouse. *Proc Natl Acad Sci USA* 97: 883–888, 2000.

Parsons TD, Lenzi D, Almers W, Roberts WM. Calcium-triggered exocytosis and endocytosis in an isolated presynaptic cell: capacitance measurements in saccular hair cells. *Neuron* 13: 875–883, 1994.

Postlethwaite M, Hennig MH, Steinert JR, Graham BP, Forsythe ID. Acceleration of AMPA receptor kinetics underlies temperature-dependent changes in synaptic strength at the rat calyx of Held. *J Physiol* 579: 69–84, 2007.

Price GD, Trussell LO. Estimate of the chloride concentration in a central glutamatergic terminal: a gramicidin perforated-patch study on the calyx of Held. *J Neurosci* 26: 11432–11436, 2006.

Rieke F, Schwartz EA. Asynchronous transmitter release: control of exocytosis and endocytosis at the salamander rod synapse. *J Physiol* 493: 1–8, 1996.

Rizzoli SO, Jahn R. Kiss-and-run, collapse and "readily retrievable" vesicles. *Traffic* 8: 1137–1144, 2007.

Roos J, Kelly RB. The endocytic machinery in nerve terminals surrounds sites of exocytosis. *Curr Biol* 9: 1411–1414, 1999.

Sakaba T. Roles of the fast-releasing and the slowly releasing vesicles in synaptic transmission at the calyx of held. *J Neurosci* 26: 5863–5871, 2006.

Sakaba T, Neher E. Calmodulin mediates rapid recruitment of fast-releasing synaptic vesicles at a calyx-type synapse. *Neuron* 32: 1119–1131, 2001a.

Sakaba T, Neher E. Preferential potentiation of fast-releasing synaptic vesicles by cAMP at the calyx of Held. *Proc Natl Acad Sci USA* 98: 331–336, 2001b.

Sakaba T, Neher E. Involvement of actin polymerization in vesicle recruitment at the calyx of Held synapse. *J Neurosci* 23: 837–846, 2003.

Sätzler K, Sohl LF, Bollmann JH, Borst JG, Frotscher M, Sakmann B, Lubke JH. Three-dimensional reconstruction of a calyx of Held and its postsynaptic principal neuron in the medial nucleus of the trapezoid body. *J Neurosci* 22: 10567–10579, 2002.

Scheuss V, Schneggenburger R, Neher E. Separation of presynaptic and postsynaptic contributions to depression by covariance analysis of successive EPSCs at the calyx of held synapse. *J Neurosci* 22: 728–739, 2002.

Schweizer FE, Ryan TA. The synaptic vesicle: cycle of exocytosis and endocytosis. *Curr Opin Neurobiol* 16: 298–304, 2006.

Smillie KJ, Evans GJ, Cousin MA. Developmental change in the calcium sensor for synaptic vesicle endocytosis in central nerve terminals. *J Neurochem* 94: 452–458, 2005.

Smith C, Neher E. Multiple forms of endocytosis in bovine adrenal chromaffin cells. *J Cell Biol* 139: 885–894, 1997.

Südhof TC. The synaptic vesicle cycle. *Annu Rev Neurosci* 27: 509–547, 2004.

Sun JY, Wu LG. Fast kinetics of exocytosis revealed by simultaneous measurements of presynaptic capacitance and postsynaptic currents at a central synapse. *Neuron* 30: 171–182, 2001.

Sun JY, Wu XS, Wu LG. Single and multiple vesicle fusion induce different rates of endocytosis at a central synapse. *Nature* 417: 555–559, 2002.

Taschenberger H, Leao RM, Rowland KC, Spirou GA, von Gersdorff H. Optimizing synaptic architecture and efficiency for high-frequency transmission. *Neuron* 36: 1127–1143, 2002.

Taschenberger H, von Gersdorff H. Fine-tuning an auditory synapse for speed and fidelity: developmental changes in presynaptic waveform, EPSC kinetics, and synaptic plasticity. *J Neurosci* 20: 9162–9173, 2000.

Teng H, Cole JC, Roberts RL, Wilkinson RS. Endocytic active zones: hot spots for endocytosis in vertebrate neuromuscular terminals. *J Neurosci* 19: 4855–4866, 1999.

Teng H, Wilkinson RS. Clathrin-mediated endocytosis near active zones in snake motor boutons. *J Neurosci* 20: 7986–7993, 2000.

Teng H, Wilkinson RS. "Delayed" endocytosis is regulated by extracellular Ca^{2+} in snake motor boutons. *J Physiol* 551: 103–114, 2003.

Teng H, Wilkinson RS. Clathrin-mediated endocytosis in snake motor terminals is directly facilitated by intracellular Ca^{2+}. *J Physiol* 565: 743–750, 2005.

Trommershauser J, Schneggenburger R, Zippelius A, Neher E. Heterogeneous presynaptic release probabilities: functional relevance for short-term plasticity. *Biophys J* 84: 1563–1579, 2003.

von Gersdorff H, Borst JG. Short-term plasticity at the calyx of Held. *Nat Rev Neurosci* 3: 53–64, 2002.

von Gersdorff H, Matthews G. Dynamics of synaptic vesicle fusion and membrane retrieval in synaptic terminals. *Nature* 367: 735–739, 1994.

von Gersdorff H, Schneggenburger R, Weis S, Neher E. Presynaptic depression at a calyx synapse: the small contribution of metabotropic glutamate receptors. *J Neurosci* 17: 8137–8146, 1997.

Wadel K, Neher E, Sakaba T. The coupling between synaptic vesicles and Ca^{2+} channels determines fast neurotransmitter release. *Neuron* 53: 563–575, 2007.

Wang LY, Kaczmarek LK. High-frequency firing helps replenish the readily releasable pool of synaptic vesicles. *Nature* 394: 384–388, 1998.

Wolfel M, Lou X, Schneggenburger R. A mechanism intrinsic to the vesicle fusion machinery determines fast and slow transmitter release at a large CNS synapse. *J Neurosci* 27: 3198–3210, 2007.

Wolfel M, Schneggenburger R. Presynaptic capacitance measurements and Ca^{2+} uncaging reveal submillisecond exocytosis kinetics and characterize the Ca^{2+} sensitivity of vesicle pool depletion at a fast CNS synapse. *J Neurosci* 23: 7059–7068, 2003.

Wu LG. Kinetic regulation of vesicle endocytosis at synapses. *Trends Neurosci* 27: 548–554, 2004.

Wu SH, Kelly JB. Response of neurons in the lateral superior olive and medial nucleus of the trapezoid body to repetitive stimulation: intracellular and extracellular recordings from mouse brain slice. *Hear Res* 68: 189–201, 1993.

Wu W, Wu LG. Rapid bulk endocytosis and its kinetics of fission pore closure at a central synapse. *Proc Natl Acad Sci USA* 104: 10234–10239, 2007.

Wu W, Xu J, Wu XS, Wu LG. Activity-dependent acceleration of endocytosis at a central synapse. *J Neurosci* 25: 11676–11683, 2005.

Wu XS, Xue L, Mohan R, Paradiso K, Gillis KD, Wu LG. The origin of quantal size variation: vesicular glutamate concentration plays a significant role. *J Neurosci* 27: 3046–3056, 2007.

Yamashita T, Hige T, Takahashi T. Vesicle endocytosis requires dynamin-dependent GTP hydrolysis at a fast CNS synapse. *Science* 307: 124–127, 2005.

Yang YM, Wang LY. Amplitude and kinetics of action potential-evoked Ca^{2+} current and its efficacy in triggering transmitter release at the developing calyx of held synapse. *J Neurosci* 26: 5698–5708, 2006.